4-15-2010

Nanostructured Poly(3,4-Ethylenedioxythiophene)–Metalloporphyrin Films: Improved Catalytic Detection of Peroxynitrite

Serban Peteu
Cleveland State University

Pubudu Peiris
Clevland State University

Ermias Gebermichael
Cleveland State University

Mekki Bayachou
Cleveland State University, M.BAYACHOU@csuohio.edu

Nanostructured poly(3,4-ethylenedioxythiophene)–metalloporphyrin films: Improved catalytic detection of peroxynitrite

Serban Peteu , Pubudu Peiris, Ermias Gebremichael, Mekki Bayachou

Introduction

Peroxynitrite ($ONOO^-$), a product of the reaction of nitric oxide with superoxide, is a potent and versatile oxidative and nitrosative agent. This cytotoxic agent is linked to a host of patho-physiological conditions and is also emerging as a possible physiological regulator. There is a growing interest in evaluating its role as an oxidation and nitration agent of a number of biological targets, which triggers a parallel increase in the need to accurately quantify this reactive analyte. Methods based on electrochemical detection are faster, simpler, and usually provide a reliable quantification. ONO_2^- is a short-lived species under physiological conditions, with $t_{1/2} \cong 1$ s at $T = 25\,^\circ$C for pH = 7.4, decomposing via the intermediate form of its conjugated acid ONO_2H ($pK_a = 6.8$) as shown by Kissner et al. (1997). Nevertheless, it displays a wide range of biochemical reactivity, since it has been shown to (i) nitrate proteins, carbohydrates, and nucleic acids; (ii) to oxidize lipids, thiol groups, Fe/S and Zn/S centers (Beckman et al., 1994) and (iii) to freely cross the cytoplasmic membrane of red blood cells when protonated (Radi, 1998). Consequently, ONO_2^- has been associated with several pathological conditions such as arthritis, inflammation, apoptosis, ageing, Huntington and Parkinson diseases, AIDS, and acute ischemia–reperfusion injury (Groves, 1999; Salvemini et al., 1998). In biological systems, superoxide $O_2^{\bullet -}$ and nitric oxide $NO^\bullet$ couple at a rate constant close to the diffusion limit, to form peroxynitrite:

$$NO^\bullet + O_2^{\bullet -} \rightarrow ONO_2^- \quad (1)$$

The typical detection methods for peroxynitrite: oxidation of fluorescent probes, EPR spectroscopy, chemiluminescence, immunohistochemistry, and probe nitration, are more difficult to apply for its real-time quantification, due to their inherent complexity.

Most recently published detection methods for peroxynitrite, if not all, are fluorescent (Cao et al., 2005; Du and Guo, 2008; Huang et al., 2007; Martin-Romero et al., 2004; Panizzi et al., 2009; Sun et al., 2009; Zheng et al., 2006; Yang et al., 2006).

The electrochemical technique is a faster, simpler, and more convenient quantification method able to monitor transient concentration changes of this reactive analyte. In a series of investigation aiming at finding a suitable electrocatalyst for peroxynitrite, we found that hemin catalyzes peroxynitrite's oxidation (see Supporting Information, Figures S1 and S2). Amatore's group (Amatore et al., 2001) studied the electrochemical signature of peroxynitrite oxidation by steady-state and transient voltammetry and used it in the quantitation of this species as released by single human fibroblasts. Another research outlined the sensitive and selective detection of peroxynitrite anion, released from cultured neonatal myocardial cells induced by ischemia–reperfusion,

based on its electrocatalytic reduction (Xue et al., 2000). Furthermore, advances are reported in using electroactive polymers (such as polypyrrole, polyaniline or polythiophene) in (bio)analytical electrochemical sensors. These 'synthetic metals' exhibit rather unique properties, including mediating rapid electron transfer and direct communication, added to their ability to be synthesized under mild conditions, and deposited onto conductive surfaces from monomer solutions with precise electrochemical control of their formation rate and thickness (Wallace et al., 1999; Vidal et al., 2003). In our effort to improve the sensitivity or our bare hemin electrodes, we set out to investigate the quantification of peroxynitrite using carbon fiber microelectrodes modified with poly(3,4-ethylenedioxythiophene)-functionalized hemin.

Materials and methods

Peroxynitrite synthesis

Peroxynitrite was synthesized in house, using the two-phase displacement reaction with the hydroperoxide anion in the aqueous phase and the isoamyl nitrite in the organic phase (Uppu and Pryor, 1996). The product, peroxynitrite, remained in the aqueous phase, whereas the isoamyl alcohol formed in the organic phase along with the unreacted isoamyl nitrite. The aqueous phase contained some isoamyl alcohol and the unreacted hydrogen peroxide, but only residual traces, if any, of isoamyl nitrite. Removal of isoamyl alcohol, and any traces of isoamyl nitrite, was accomplished by washing the aqueous phase with dichloromethane and chloroform. The hydrogen peroxide was removed by passing the solutions through a manganese dioxide column. The peroxynitrite, with a final concentration of up to 850 mM, was stored in 5 mL aliquots at −80 °C. Its concentration was assessed by UV–vis at 302 nm, using the molecular absorbtivity $\varepsilon_{302} = 1705\ \mathrm{mol^{-1}\ cm^{-1}}$ both before and after every analytical test. During these experiments, analyte solutions are kept on ice to minimize the spontaneous peroxynitrite decay throughout all experiments.

Chemicals

The iron protoporphyrin IX (hemin), the protoporphyrin and the 3,4-ethylenedioxythiophene (EDOT) were purchased from Sigma–Aldrich, St. Louis, MO. The deionized (DI) water was from a Barnstead ultrapure water system Model D8961 with the water resistivity of at least 18.2 MΩ cm. All other chemicals were reagent grade and were used as received.

Preparation of hemin-modified carbon fiber electrodes

The 30-μm diameter glass-encased carbon fiber microelectrodes (CFEs) were prepared using published methods, described in detail elsewhere (Kawagoe et al., 1993). The films of electropolymerized porphyrins were deposited on freshly cleaned carbon fiber electrodes. Prior to coating, electrodes were sonicated in ethanol–acetone for 3 min and gently dried with pure nitrogen. The hemin films were electropolymerized from a solution of 1.5 mM hemin monomer, in the presence of 0.1 M tetrabutylammonium tetrafluoroborate in dichloromethane (Younathan et al., 1992). After each modification, the electrode was rinsed, the electrodeposited film being gently flushed with organic and aqueous solvents, to remove excess material, allowed to dry and then was ready to use. The preparation of the hemin–PEDOT modified carbon fiber microelectrodes is similar, as will be outlined later in the text.

Apparatus and procedures

The cyclic voltammetry experiments were performed in a three-electrode configuration cell on a BAS 100B electrochemical workstation. All electrochemical experiments were performed at room temperature 24 ± 2 °C. Unless otherwise noted, the working electrode was polarized a 750 mV vs. Ag/AgCl reference, and all test were run in 100 mM CAPS pH 10.5 buffer solution. The Ag/AgCl electrode was used as the reference electrode, and all potentials reported here are vs. this reference. A platinum wire was used as the auxiliary, and the working electrode (WE) was the carbon fiber. The time-based amperometric dose–response tests were performed using the CHI Instruments electrochemical station Model 440 with the same electrochemical cell, the WE being polarized at 750 mV unless otherwise noted. Just before use, a sealed flask containing the peroxynitrite stock solution was allowed to thaw at room temperature and then kept on ice. Oxygen was removed by purging with N_2 for at least 30 min. Peroxynitrite aliquots were added with a gastight syringe, from the sealed flask under the N_2 blanket. Any dilutions were made fresh just before use, in the same de-oxygenated buffer. All graphed data points represent an average of at least three different experiments, unless mentioned otherwise. The morphology of the porphyrin films and bare CFEs were imaged up to 100k magnification, with the FESEM Hitachi S-4500.

Results and discussion

Our studies on hemin polymerized films acting as electrocatalysts for peroxynitrite oxidation, although promising, showed that there is ample room for improvement of sensitivity (Supporting Information, Figures S1 and S2). Elsewhere, carbon-based electrodes were functionalized with electroactive polymers such as polyaniline, polypyrrole or polythiophene, and used for electrochemical sensing. In an effort to increase the sensitivity of our hemin-modified carbon fiber electrodes (CFEs), we set out to investigate the inherently conductive poly(3,4-ethylenedioxythiophene) (PEDOT) functionalized with hemin, by electrodeposition on a 30-μm diameter CFE. There are previous reports of electroactive polymers such as polypyrrole or polyaniline in (bio)analytical electrochemical sensors (Wallace et al., 1999; Vidal et al., 2003). These 'synthetic metals' exhibit high conductivity, mediate rapid electron transfer and can be synthesized under mild conditions through simple deposition onto conductive surfaces from monomer solutions with precise electrochemical control. By comparison with polypyrrole, PEDOT seems to show a better electrochemical stability, with a better conservation of its conductivity and charge. Also, polythiophenes have a higher ionization potential compared to polypyrroles, *ca.* 5 eV vs. 4 eV, protecting these against the oxidative damage by the oxygen in the air (Micaroni et al., 2002).

Preparation for the PEDOT-functionalized hemin CFEs

The hemin–PEDOT solution was prepared with 1.5 mM hemin monomer, 4.5 mM monomer EDOT, and 0.1 M tetrabutylammonium tetrafluoroborate in dichloromethane. For hemin–PEDOT electrodeposition, ensuing increases in the redox peak currents were recorded, scanning for 10 cycles between −1.6 V and 1.6 V, four times, as seen in Supporting Information, Figure S3. From the constant increase in peak currents, it could be concluded that an electroactive, superimposed multi-layered matrix was deposited and growing on the electrode's surface, capable of mediating the electrolysis of incoming porphyrin monomer at the film–solution interface. For hemin–PEDOT electrodeposition, ensuing increases in the redox peak currents were recorded. In the case of the hemin

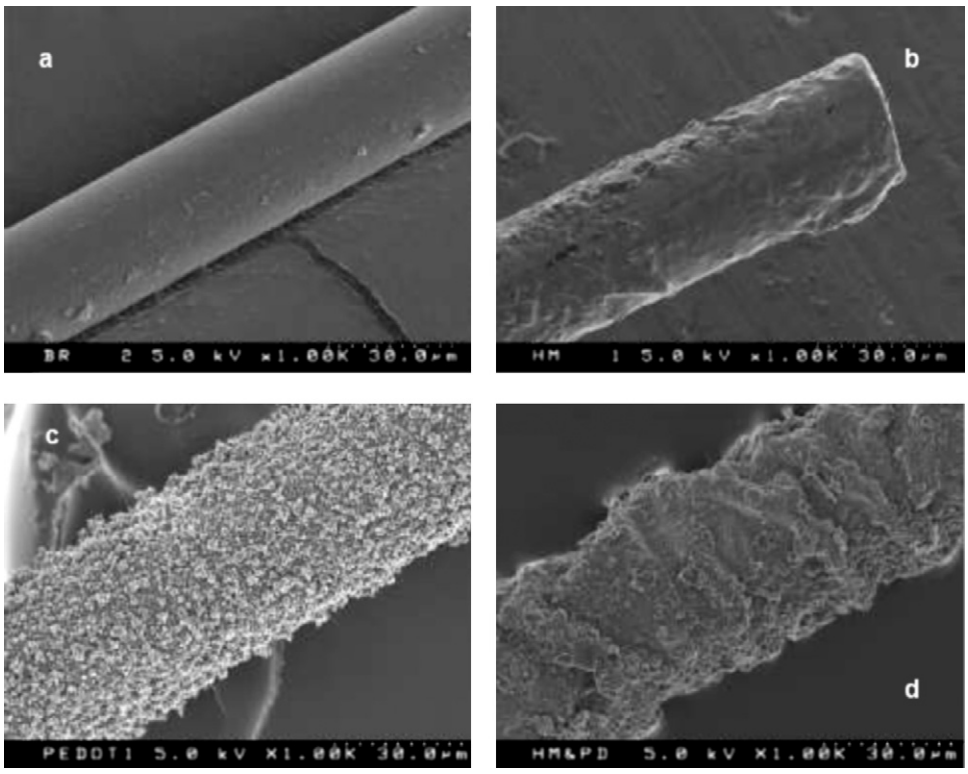

Fig. 1. SEM images of CFEs: bare (a); hemin modified (b); PEDOT only CFE (c); and hemin–PEDOT modified CFE (d). All images were obtained at 5 kV and with 1k magnification with bar length of 30 μm.

solution, the surface coverage increased gradually through the first 10–15 scans, then the electronic migration through the layer was attenuated by the existing hemin film layer, and the rate of further hemin growth almost stops, and for the 15th scan or so, the growth completely ceases. By contrast, the PEDOT–hemin multilayered matrix exhibited an uninterrupted and constant growth, with rather uniform increase in its peak currents for at least the first 40 scans. The inherent, relative high conductivity of the polythiophene polymeric film should be responsible for this continuous, constant growth of the PEDOT–hemin layer. This difference between the hemin film and the PEDOT–hemin is also apparent from their surface morphology, imaged with FESEM, as will be shown below.

Surface characterization

Scanning electron microscopy (SEM) was utilized to image the morphology of the active surface of the electrodeposited hemin films with and without PEDOT, and compared with the bare carbon fiber, as shown in Fig. 1a–d. The bare CFE appears flat, in contrast with the hemin electropolymerized film, which has a relatively smooth surface with thin electrodeposited film with an apparent thickness on the radius, $\Delta R = 2.75\ \mu m$, as determined by optical microscopy (figure not shown). For the early stages of hemin electropolymerization, the surface defects may be used as nucleation sites. These nascent nano-grains tend to coalesce into bigger micro-islands. By comparison, the hemin–PEDOT polymerized layer is much thicker, measuring $\Delta R = 9\ \mu m$ on the radius, and its surface is extremely fractal and rough with peaks and valleys—at microscale. Further nano-scale magnification up to 10,000× from Fig. 2 reveals a typical nanostructured 'cauliflower', that is a 3D branched-multiglobular surface with features with dimensions mostly in the 100–300 nm range. The PEDOT surface with $\Delta R = 9\ \mu m$ appears more uniform than hemin–PEDOT, and the microscale has quasi-pyramidal, sharp protrusions.

The X-ray energy dispersive spectroscopy (XEDS) spectra for the hemin–PEDOT and protoporphyrin–PEDOT are both showing the sulfur peak (S = 16–19.7 wt%) characteristic of PEDOT, as seen in Fig. 3. The iron peak is present in hemin–PEDOT (Fe = 2.3 wt%), but absent for our control with protoporphyrin–PEDOT where the iron metal center is lacking (Fe = 0.0 wt%).

The XEDS was used as a sensitive analytic tool to study and ascertain the surface composition of the catalyst layers. The X-rays penetrate a substantial distance into the sample and excite electrons (photoelectrons). A small fraction of these electrons from the top 5 nm film make it outside and are detected, in terms of their kinetic energy. The XEDS spectra for the hemin–PEDOT and protoporphyrin–PEDOT are both showing the sulfur peak (S = 16–19.7 wt%) characteristic of PEDOT, Fig. 3. The iron peaks are definitely present in hemin–PEDOT (Fe = 2.3 wt%) matrix, but completely absent for the protoporphyrin–PEDOT (Fe = 0.0 wt%) matrix.

Response of the hemin-modified electrode to peroxynitrite

. *Cyclic voltammetry*

The typical cyclic voltammetric response of the electropolymerized hemin and hemin–PEDOT films is shown in Fig. 4. As previously reported, the hemin-modifed CFE from Fig. 5A showed a constant increase of the oxidation peak current for different aliquots of peroxynitrite subsequently added to the stirred cell, with the current in the tens of μA range. A typical hemin–PEDOT modifed CFE from Fig. 5B had its oxidation peak current also proportional with the ONO_2^- concentration. The main oxidation peak, assigned to PEDOT, is close to 0 (zero) mV which indicates the potential of detecting peroxynitrite with the electrode at 0 (zero) polarization in time-based amperometry. This is conducive of removing the interference of the potential competing substrates that would oxidize in the region 100–700 mV. The second oxidation peak at 1250 mV, characteristic of hemin, is more visible for ONO_2^- concentrations higher than 300 μM.

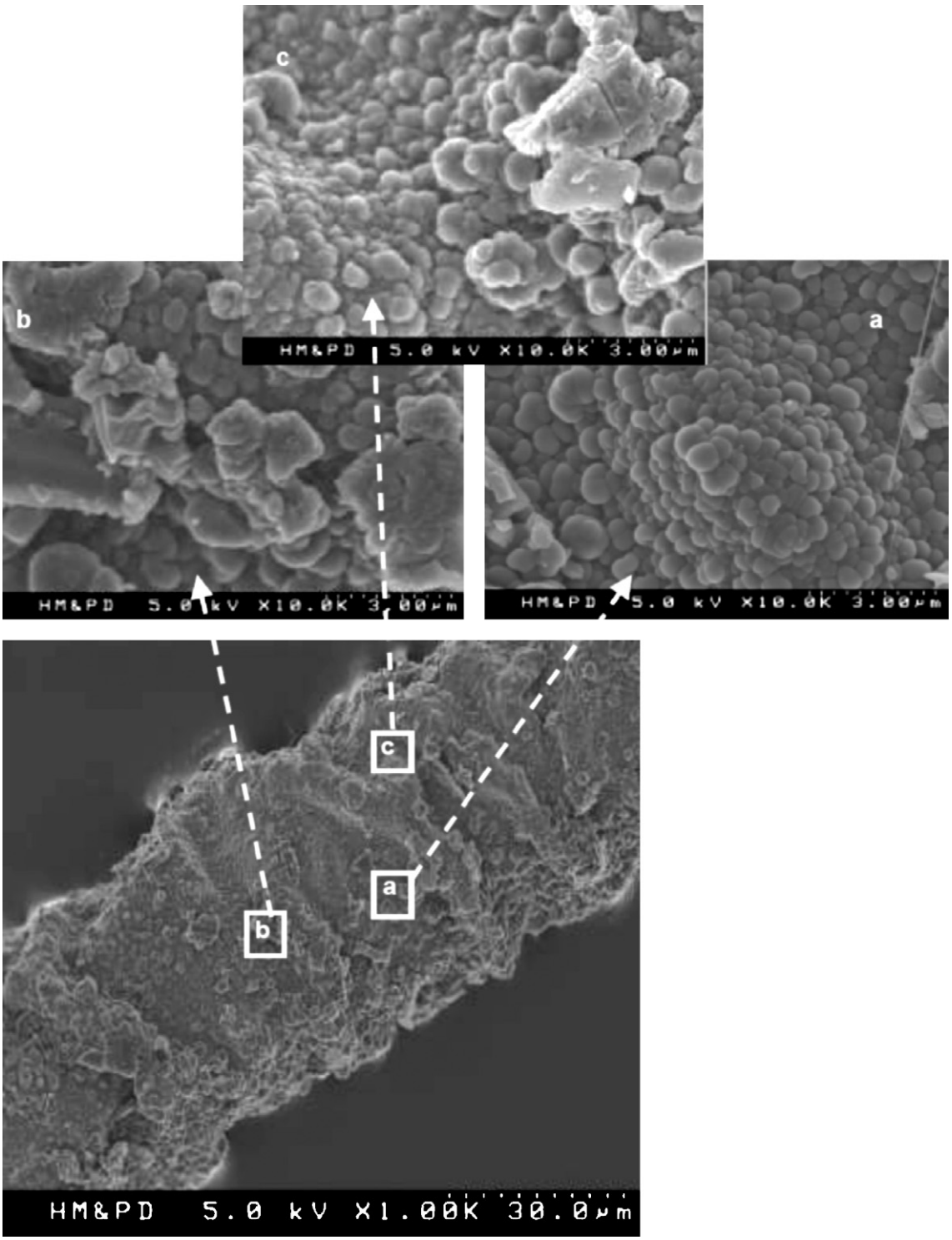

Fig. 2. FESEM of a typical hemin–PEDOT modified CFE showing a typical wavy and wrinkled edgy micro-structure, with numerous 'cauliflower'-type nano-grains (a–c). Images (a)–(c) taken at 5 kV with 10k magnification with bar length of 3 μm.

pH dependence

In a previous work, we found that hemin-based carbon electrodes oxidation peak potential depend strongly on the buffer's pH (Supporting Information, Figure S1). In addition, Peroxynitrite is relatively unstable and is known to decay both through isomerization and decomposition at various pHs and temperatures (Kissner and Koppenol, 2002). The performance characterization at low pHs (*ca.* 7.6), although possible is difficult because of the complexity that the inherent decay brings. To characterize the intrinsic response of our hemin–PEDOT microsensors, we focused mainly on the pH were peroxynitrite was the most stable, i.e. pH 10.5 CAPS buffer, since we were concerned only with the investigation and analytical characterization of our hemin–PEDOT CFEs as a platform to detect peroxynitrite. However, for comparison purposes, we report in supporting information (Figure S4) the response of a typical hemin–PEDOT microelectrode decreases at lower pHs.

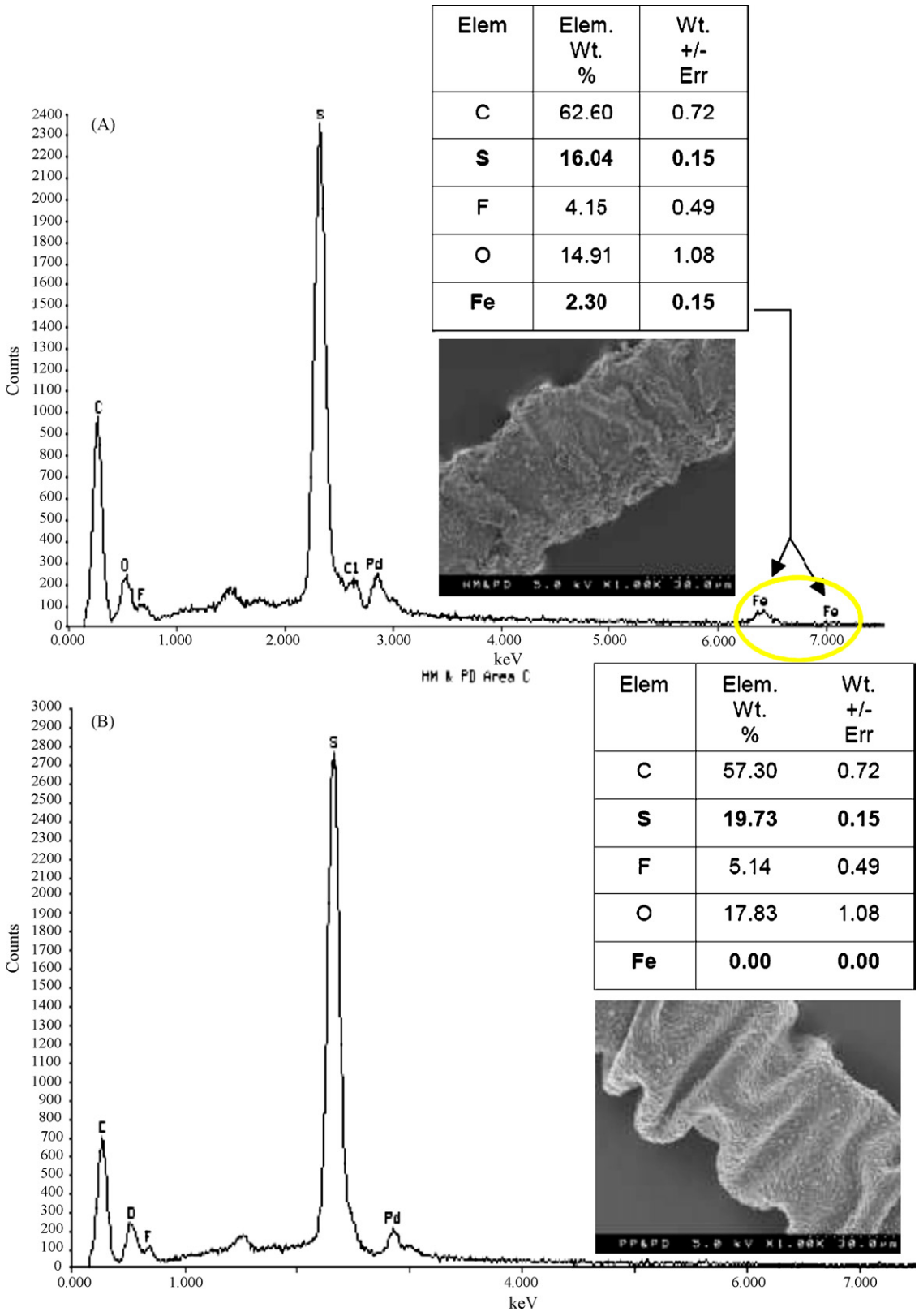

Elem	Elem. Wt. %	Wt. +/- Err
C	62.60	0.72
S	**16.04**	**0.15**
F	4.15	0.49
O	14.91	1.08
Fe	**2.30**	**0.15**

Elem	Elem. Wt. %	Wt. +/- Err
C	57.30	0.72
S	**19.73**	**0.15**
F	5.14	0.49
O	17.83	1.08
Fe	**0.00**	**0.00**

Fig. 3. XEDS spectra for the typical hemin–PEDOT and protoporphyrin–PEDOT, showing the sulfur peak (S = 16–19.7 wt%) characteristic of PEDOT and the iron peak (Fe = 2.3 wt%) present in hemin–PEDOT, but absent for protoporphyrin–PEDOT.

While the response of the electrode decreases at lower pHs, the decrease is mainly due to inherent decay of the analyte and is in line with known decay/isomerization schemes PON under these conditions (Kissner and Koppenol, 2002).

Amperometry

To further evaluate the electrochemical characteristics of the hemin–PEDOT modified carbon fiber as potential peroxynitrite-sensitive electrodes, several time-based amperometry tests were

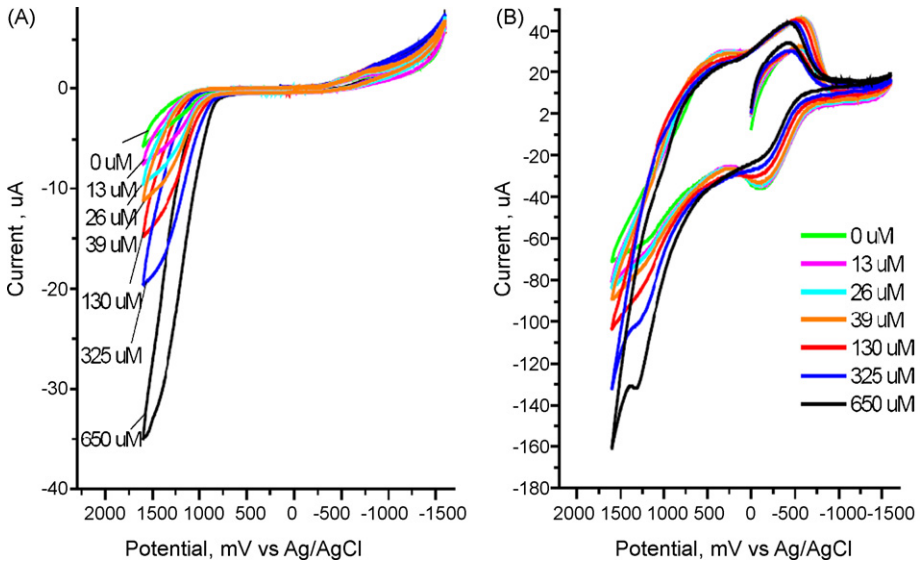

Fig. 4. Cyclic voltammogram at 150 mV/s, with 750 mV polarization vs. Ag/AgCl reference, in pH 10.5 CAPS buffer solution for hemin modified (A) and hemin–PEDOT modifed (B), after addition of different ONO_2^- aliquots.

performed. The current was measured in response to varying amounts of peroxynitrite standard solution, successively added to magnetically stirred, deaerated 10.5 pH buffer solution. A typical dose–response current trace is shown in Fig. 6. Each arrow indicates when a ONO_2^- aliquot was added to this solution. The typical time-based amperometric response of the hemin–PEDOT modified CFEs is compared with the PEDOT CFE, hemin CFE and bare CFE.

The calibration curves from these amperometric tests are shown in Fig. 6A with a focus (zoom) on for 0–40 μM analyte concentration range. We also performed amperometric tests with lower concentrations of peroxynitrite solutions to determine the limit of detection, Fig. 6B.

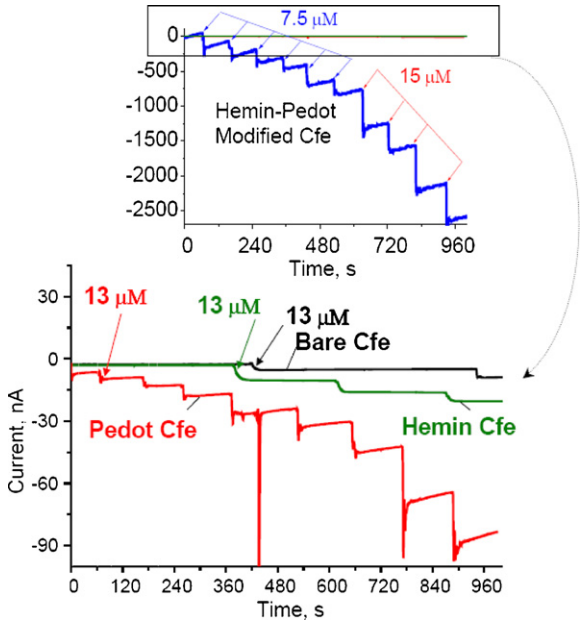

Fig. 5. The time-based amperometric typical response of the hemin–PEDOT modified CFEs, compared with the PEDOT CFE, the hemin CFE and the bare CFE. All polarized at 750 mV vs. Ag/AgCl reference, in pH 10.5 CAPS buffer solution.

Based on responses obtained with analyte concentration in nanomolar range, the limit of detection based, on the 3-to-1 response-to-noise ratio criterion, was determined to be 200 nM peroxynitrite. The typical 90% response times for the modified carbon fiber electrodes were between 5 s and 30 s, depending on the fiber length, and the thickness of the catalyst film, which in turn depends on the duration of the electrodeposition.

Repeatability, reproducibility, and interference

We have investigated repeatability and reproducibility of the response of our hemin–PEDOT to added PON aliquots. Overall, we show a good degree of response repeatability of the sensor from one addition to another and over several peroxynitrite concentrations (see for instance Figs. 5 and 6B). Also, electrodes constructed and stored under the same conditions give reproducible responses in response to added peroxynitrite. A graph featuring typical response variability with four different tests each is shown in Supporting Information (Figure S5).

The main decomposition products of peroxinitrite are nitrite and nitrate with a product distribution that depends on factors such as pH and temperature. We have tested the response of our modified electrodes towards peroxynitrite as compared to the response of nitrite and nitrate. Figure S6 shows typical responses of these possible interferences and shows that our modified electrodes are very inherently selective and more responsive to equimolar additions of PON. It is worth mentioning that the response of our PON sensors is essentially stable as concluded from response monitoring of a typical electrode over two weeks (see Figure S7, Supporting Information)

Future work

Work is now underway to test the performance of our hemin–PEDOT microelectrodes *in vitro* on recombinant nitric oxide synthase (NOS) enzymes with various degrees of coupling of NAPDH consumption to nitric oxide synthesis; the uncoupling results in a direct formation of peroxynitrite as a side product, which can therefore be used as a marker for this enzymatic dysfunction.

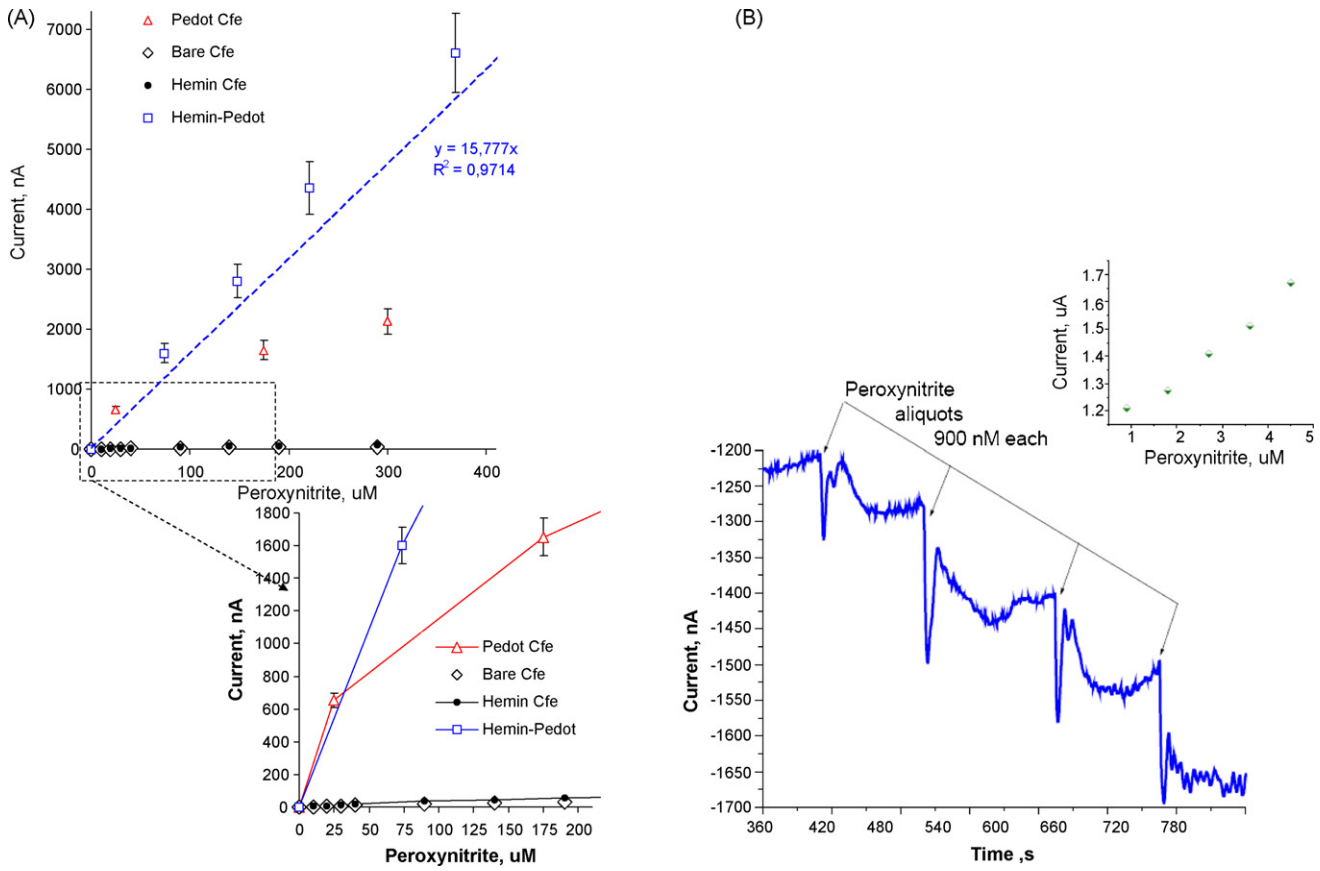

Fig. 6. (A) The calibration curves based on time-based amperometric data for the hemin–PEDOT modified CFEs, compared with the PEDOT CFE, the hemin CFE and the bare CFE. Polarization at 750 mV vs. Ag/AgCl reference, in pH 10.5 CAPS buffer solution. (B) Time-based amperometric test with diluted peroxynitrite for the limit of detection. Polarization at 750 mV vs. Ag/AgCl reference, in pH 10.5 CAPS buffer solution.

Conclusions

In this paper, we investigated hemin–PEDOT CFEs in effort to prepare an efficient sensing platform for peroxynitrite. The addition of PEDOT as an electroactive polymer with high conductivity, would mediate a rapid electron transfer, in addition to improving the electrodeposition of the hemin–EDOT monomers with precise electrochemical control. The electrocatalytic oxidation of peroxynitrite was characterized by cyclic voltammetry, indicating an increase of the catalytic current as a function of analyte's concentration. The data presented herein seem to fully support the "synergy" hypothesis between the conductive PEDOT matrix and hemin electrocatalyst. Our composite hemin–PEDOT films were revealed as fractal 3D matrices with inherent tortuous peak-and-valley nanostructured surfaces. The highly tortuous catalytic platform implies that an analyte molecule must travel a longer path through the twisted, bent pores, from the outer film surface to inner catalytic sites on the hemin–PEDOT film. Consequently, these results in larger contact surface between the catalyst and the analyte, and, consequently, increase in the ratio current-to-analyte concentration, hence a higher sensitivity. In conclusion, optimized hemin–PEDOT modified CFEs were utilized for the first time to detect ONO_2^-, with a response time down to 5 s and a limit of detection as low as 200 nM as evidenced by the time-based dose–response amperometry. For the first time, to the best of our knowledge, these hemin–PEDOT modified CFEs showed a sensitivity of 13 nA/μM (or 13 pA/nM), 52 times higher than the hemin-modified CFE and 130 times higher than the bare CFE. We are also exploring other electrocalalysts to improve the detection limit, the selectivity, and to further miniaturize the hemin–PEDOT modified electrodes.

Acknowledgements

This research was supported by the National Science Foundation (MB; Grant CHE-0848820) and by an FRD and seed grants from CSU-Ohio Board of Regents.

Appendix A. Supplementary data

Supplementary data associated with this article can be found, in the online version, at doi:10.1016/j.bios.2010.01.008.

References

Amatore, C., Arbault, S., Bruce, D., de Oliveira, P., Erard, M., Vuillaume, M., 2001. Chemistry: A European Journal 7 (19), 4171–4179.
Beckman, J.S., Chen, J., Ischiropoulos, H., Crow, J.P., 1994. Methods in Enzymology 233, 229–240.
Cao, Q.H., Zhou, Q.X., Cai, R.X., et al., 2005. Analytical Sciences 21 (4), 445–447.
Du, J.O., Guo, X.Q., 2008. Spectroscopy and Spectral Analysis 28 (8), 1875–1878.
Groves, J.T., 1999. Current Opinion in Chemical Biology 3 (2), 226–235.
Huang, J.C., Li, D.J., Diao, J.C., et al., 2007. Talanta 72 (4), 1283–1287.
Kawagoe, K.T., Zimmerman, J.B., Whightman, R.M., 1993. Journal of Neuroscience Methods 48, 228–240.
Kissner, R., Nauser, T., Bugnon, P., Lye, P.G., Koppenol, W.H., 1997. Chemical Research in Toxicology 10 (11), 1285–1292.
Kissner, R., Koppenol, W.H., 2002. Journal of the American Chemical Society 124 (2), 234–239.
Martin-Romero, F.J., Gutierrez-Martin, Y., Henao, F., et al., 2004. Journal of Fluorescence 14 (1), 17–23.
Micaroni, L., Nart, F.C., Hummelgen, I.A., 2002. Journal of Solid State Electrochemistry 7 (1), 55–59.
Panizzi, P., Nahrendorf, M., Wildgruber, M., et al., 2009. Journal of the American Chemical Society 131 (43), 15739–15744.
Radi, R., 1998. Chemical Research in Toxicology 11 (7), 720–721.

Salvemini, D., Jensen, M.P., Riley, D.P., Misko, T.P., 1998. Drug News and Perspectives 11 (4), 204–214.
Sun, Z.N., Wang, H.L., Liu, F.Q., et al., 2009. Organic Letters 11 (9), 1887–1890.
Uppu, R.M., Pryor, W.A., 1996. Analytical Biochemistry 236, 242–249.
Vidal, J.-C., Garcia-Rui, E., Castillo, J.-R., 2003. Microchimica Acta 143 (2–3), 93–111.
Wallace, G.G., Smyth, M., Zhao, H., 1999. TRAC-Trends in Analytical Chemistry 18 (4), 245–251.
Xue, J., Ying, X.Y., Chen, J.S., Xian, Y.H., Jin, L.T., Jin, J., 2000. Analytical Chemistry 72 (21), 5313–5321.
Yang, D., Wang, H.L., Sun, Z.N., et al., 2006. Journal of the American Chemical Society 128 (18), 6004–6005.
Younathan, J.N., Wood, K.S., Meyer, T.J., 1992. Inorganic Chemistry 31 (15), 3280–3285.
Zheng, Q., Qiu, F., Liu, Z.H., et al., 2006. Chinese Journal of Analytical Chemistry 34 (1), 26–30.